Measurement of the dielectron continuum in $p+p$ and $\mathrm{Au}+\mathrm{Au}$ collisions at RHIC

T. DAHMS, for the PHENIX Collaboration
CERN,
1211 Geneva 23, Switzerland

PHENIX has measured the e^+e^- pair continuum in $\sqrt{s_{NN}} = 200$ GeV $\mathrm{Au}+\mathrm{Au}$ and $p+p$ collisions over a wide range of mass and transverse momenta. While the $p+p$ data in the mass range below the ϕ meson are well described by known contributions from light meson decays, the $\mathrm{Au}+\mathrm{Au}$ minimum bias inclusive mass spectrum shows an enhancement by a factor of $4.7 \pm 0.4(\mathrm{stat}) \pm 1.5(\mathrm{syst}) \pm 0.9(\mathrm{model})$ in the mass range $0.15 < m_{ee} < 0.75$ GeV/c^2. At low mass ($m_{ee} < 0.3$ GeV/c^2) and high p_T ($1 < p_T < 5$ GeV/c) an enhanced e^+e^- pair yield is observed that is in qualitative agreement with hydrodynamical models of thermal photon emission with initial temperatures ranging from $T_{init} \simeq$ 300–600 MeV at times of 0.6–0.15 fm/c after the collision.

1 Introduction

Experimental results from the Relativistic Heavy Ion Collider (RHIC) have established the formation of dense partonic matter in $\mathrm{Au}+\mathrm{Au}$ collisions at $\sqrt{s_{NN}} = 200$ GeV [1]. One of the key questions has been what is the initial temperature of the created matter. Like any medium in thermal equilibrium, the quark-gluon plasma emits black-body radiation characteristic for its temperature in form of real and virtual photons, the latter ones appearing as lepton pairs (e^+e^- or $\mu^+\mu^-$). As photons and lepton pairs do not carry color charge, they do not undergo strong final state interaction while traversing the medium. Thus, they carry all their information from the time they have been created to the detector. But, because they are emitted during all stages of the collision, any measurement will be a time integrated average and the initial temperature can only be derived by comparing to models. One of the main challenges of measuring thermal photons is the huge background due to hadron decay photons. The dominant background contribution due to π^0 decays can be avoided by measuring virtual photons rather than real photons. Any process that creates a real photon can also create a virtual photon which decays into a lepton pair. The invariant mass spectrum of virtual photons created by the quark-gluon Compton scattering ($q+g \rightarrow q+\gamma^*$) is described by the Kroll-Wada equation [2]. For direct virtual photons with $p_T \gg m_{ee}$ this spectrum is proportional to $1/m_{ee}$. Also e^+e^- pairs from π^0 Dalitz decays have the same $1/m_{ee}$ shape at $m_{ee} \ll m_{\pi^0}$, but are suppressed due to the limited phase space when approaching $m_{\pi^0} = 135$ MeV/c^2. Thus, one can measure direct virtual photons above the π^0 mass where the main background source is eliminated.

2 Results

PHENIX has measured e^+e^- pairs from $p+p$ and $\mathrm{Au}+\mathrm{Au}$ collisions at $\sqrt{s_{NN}} = 200$ GeV as a function of mass and p_T. The resulting invariant mass spectra integrated over all p_T are

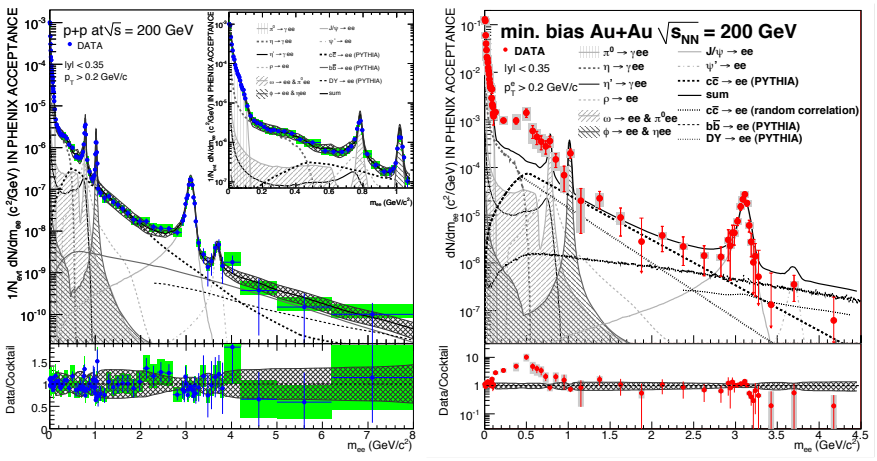

(a) (b)

Figure 1: Invariant mass distribution of e^+e^- pairs in the PHENIX acceptance in $p+p$ (a) and Au + Au (b) collisions. The data are compared to the expectations from the decays of light hadrons and correlated decays of open charm, bottom, and Drell-Yan.

shown in Fig. 1. Contributions from combinatorial and correlated background sources have been subtracted statistically utilizing mixed events and the like-sign pairs. The details of the analysis have been described in Ref.[3,4]. The p+p data are compared to a cocktail of the expected hadronic sources whose cross sections have been measured independently by PHENIX [4]. The contribution from semi-leptonic charm and bottom decays as well as Drell-Yan have been simulated with PYTHIA [5]. The agreement between data and simulation over the full mass range is excellent. By comparing the integrated yield of data and PYTHIA in the intermediate mass region of $1.1 < m_{ee} < 2.5$ GeV/c^2, which is dominated by open charm, a total charm cross section of $\sigma_{c\bar{c}} = 544 \pm 39(\text{stat}) \pm 142(\text{syst}) \pm 200(\text{model})$ μb has been measured in $p+p$ collisions. Alternatively, by fitting the normalization of the simulated shapes to the data, the charm and bottom cross sections of $\sigma_{c\bar{c}} = 518 \pm 47(\text{stat}) \pm 135(\text{syst}) \pm 190(\text{model})$ μb and $\sigma_{b\bar{b}} = 3.9(\text{stat}) \pm 2.4^{+3}_{-2}(\text{syst})$ μb, respectively, have been measured [3]. The charm cross section is in agreement with the result of the non-photon single electron measurement [6]: $\sigma_{c\bar{c}} = 567 \pm 57(\text{stat}) \pm 193(\text{syst})$ μb.

The measurement of e^+e^- pairs in Au + Au collisions is compared to the corresponding cocktail calculation in Fig. 1b. The charm contribution is the same PYTHIA calculation scaled to the number of binary collisions, N_{coll}, times the measured charm cross section of $\sigma_{c\bar{c}} = 567 \pm 57(\text{stat}) \pm 193(\text{syst})$ μb. In contrast to the p+p result, the measured yield of low mass region ($0.15 < m_{ee} < 0.75$ GeV/c^2) in minimum bias Au+Au is enhanced compared to the expectation by a factor $4.7 \pm 0.4(\text{stat}) \pm 1.5(\text{syst}) \pm 0.9(\text{model})$. The intermediate mass region is surprisingly well described by PYTHIA which is shown as dashed line in Fig. 1b. This is interesting to note, as single electron distributions from semi-leptonic charm decays show substantial medium modifications [7]. Thus, it is hard to understand how the dynamical correlation of the $c\bar{c}$ pair at production remains unaffected by the medium. An alternative scenario in which this correlation is washed out by the medium, i. e. the direction of the c and the $\bar{c}$ quark are uncorrelated, is indicated by a dotted line in the same figure. This leads to a much softer spectrum and would leave significant room for other contributions, e. g. thermal radiation emmited by quark-antiquark annihilation processes.

The p_T dependence of the low mass region ($m_{ee} < 1.2$ GeV/c^2) is shown in Fig. 2. The e^+e^- pairs measured in $p + p$ are consistent with the cocktail for the lower p_T bins. At higher p_T however, the data are above the expectation. In Au + Au the enhancement is concentrated at

low p_T but extends to the high p_T region where it is still significantly higher than in $p+p$. The shape of the low mass enhancement in Au + Au differs for $p_T < 1$ GeV/c and $p_T > 1$ GeV/c. At high p_T the excess can be interpreted as due to internal conversions of direct virtual photons which, for $p_T \gg m_{ee}$, has a well defined $1/m_{ee}$ mass dependence [2]. The data have been fit to the cocktail plus a direct photon contribution in the form of $f(m_{ee}) = (1-r)f_c(m_{ee}) + r f_{\rm dir}(m_{ee})$ with the fraction of the direct virtual photon contribution r as the free parameter. From this fraction of the direct virtual photon contribution it is possible to derive the p_T spectrum of direct real photons [8] which is shown for $p+p$ and three Au+Au centrality bins (min. bias, 0–20%, and 20–40%) in Fig. 3a. The data are extended at high p_T with the previous measurements of direct photons in the electromagnetic calorimeter of PHENIX [9,10] which are in good agreement in the overlapping p_T range. The $p+p$ data are are in good agreement with a NLO pQCD calculation of direct photons [11] which is shown for three different theory scales: $\mu = 0.5\,p_T$, p_T, and $2\,p_T$.

In order to compare the $p+p$ data quantitatively with the Au + Au measurement, the $p+p$ direct photon spectrum is fit to a modified power-law function $A_{pp}(1+p_T^2/b)^{-n}$. This fit, scaled by the nuclear overlap function T_{AA} is overlaid with the Au + Au data. For all three centrality bins the data are show a clear enhancement at low p_T. This excess is characterized by fitting the T_{AA} scaled $p+p$ fit plus an exponential $A{\rm e}^{-p_T/T} + T_{AA} \times A_{pp}(1+p_T^2/b)^{-n}$. For the 20% most central collisions, the inverse exponential slope is $T = 221 \pm 19({\rm stat}) \pm 19({\rm syst})$. The result for this centrality bin is compared in Fig. 3b to several hydrodynamical models of thermal photon emission [12,13,14,15,16,17]. The models, which assume the formation of a hot system with initial temperatures ranging from $T_{\rm init} = 300$ MeV at a thermalization time of $\tau_0 = 0.6$ fm/c to $T_{\rm init} = 600$ MeV at $\tau_0 = 0.15$ fm/c, are all in qualitative agreement with the data. Lattice QCD predicts a phase transition from the hadronic phase to the quark-gluon plasma at $T \simeq 170$ MeV.

While for $p_T > 1$ GeV/c the excess yield can be successfully described by internal conversions of direct virtual photons, the excess yield at lower p_T, which is responsible for most of the p_T integrated enhancement, shows a different mass dependence. The transverse mass dependence of the enhancement has been analysed in Ref. [4]. While not shown in this proceedings, it appears that, in addition to the thermal radiation at high m_T, there is a second much softer component at low m_T with an inverse slope of $T \sim 90$ MeV. This low mass, low p_T enhancement is currently not described by any theoretical model calculation.

References

1. K. Adcox *et al.* (PHENIX Collaboration), Nucl. Phys. **A 757**, 184 (2005).
2. N. M. Kroll and W. Wada, Phys. Rev. **98**, 1355 (1955).
3. A. Adare *et al.* (PHENIX Collaboration), Phys. Lett. **B 670**, 313 (2009).
4. A. Adare *et al.* (PHENIX Collaboration), Phys. Rev. C **81**, 034911 (2010).
5. T. Sjöstrand, *et al.*, Comp. Phys. Commun. **135**, 238 (2001).
6. A. Adare *et al.* (PHENIX Collaboration), Phys. Rev. Lett. **97**, 252002 (2006).
7. A. Adare *et al.* (PHENIX Collaboration), Phys. Rev. Lett. **98**, 172301 (2007).
8. A. Adare *et al.* (PHENIX Collaboration), Phys. Rev. Lett. **104**, 132301 (2010).
9. S. S. Adler *et al.* (PHENIX Collaboration), Phys. Rev. Lett. **94**, 232301 (2005).
10. S. S. Adler *et al.* (PHENIX Collaboration), Phys. Rev. Lett. **98**, 012002 (2007).
11. L. E. Gordon and W. Vogelsang, Phys. Rev. D **48**, 3136 (1993)
12. D. d'Enterria and D. Peressounko, Eur. Phys. J. **C 46**, 451 (2006).
13. P. Huovinen, P. V. Ruuskanen, and S. S. Rasanen, Phys. Lett. **B 535**, 109 (2002).
14. D. K. Srivastava and B. Sinha, Phys. Rev. C **64**, 034902 (2001).
15. S. Turbide, R. Rapp, and C. Gale, Phys. Rev. C **69**, 014903 (2004).
16. F. M. Liu *et al.*, Phys. Rev. C **79**, 014905 (2009).
17. Jan-e Alam *et al.*, Phys. Rev. C **63**, 021901(R) (2001).

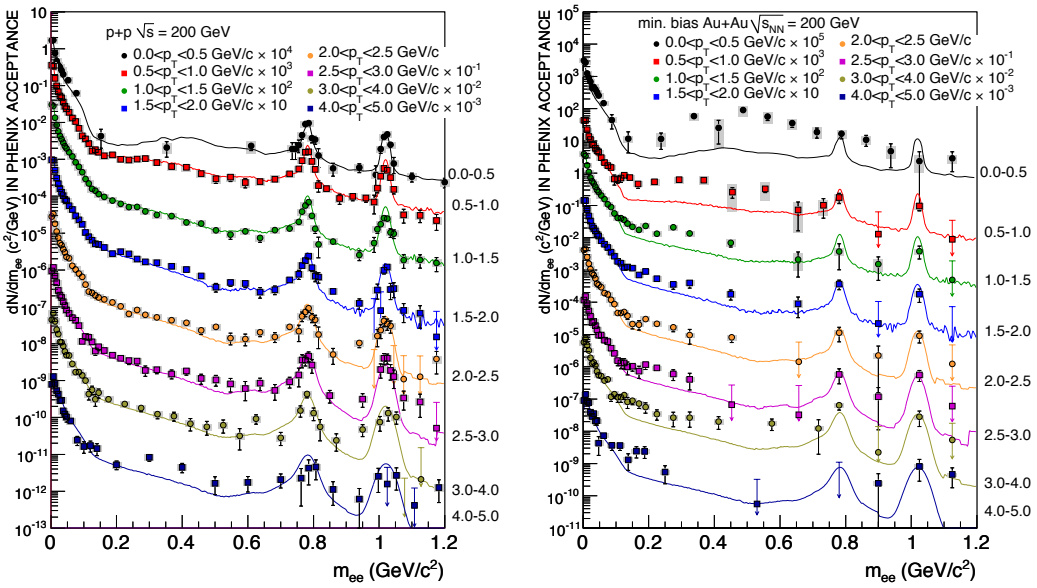

(a) (b)

Figure 2: Invariant mass distribution of e^+e^- pairs in the PHENIX acceptance for different p_T ranges in $p+p$ (a) and Au+Au (b) collisions. The data are compared to the cocktail of hadronic sources which includes the contribution from charm as described in the text.

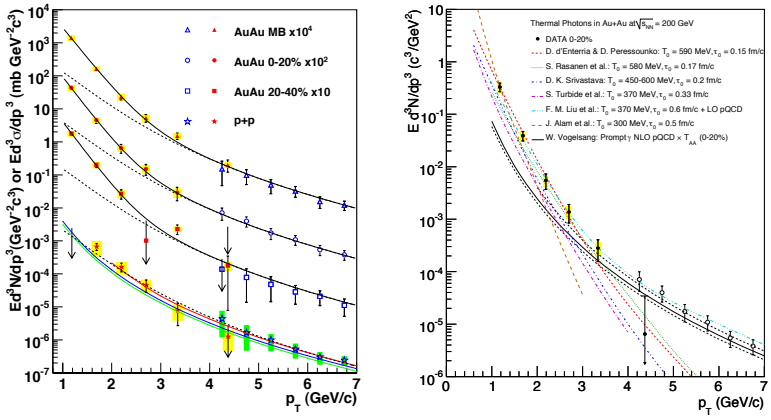

(a) (b)

Figure 3: The invariant cross section ($p+p$) and invariant yield (Au+Au) of direct photons as a function of p_T is shown in (a). Solid points are from the internal conversion analysis, open points from [9,10]. The $p+p$ data are compared to NLO pQCD calculations [11] for three theory scales $\mu = 0.5\,p_T$, p_T, and $2\,p_T$. The $p+p$ data are fit to a modified power-law (dashed curve) which is scaled by T_{AA} and compared to the Au+Au data. The Au+Au data are fitted by the T_{AA} scaled $p+p$ fit plus an exponential (solid lines). In (b) hydrodynamical model calculations of thermal photon emission are compared with the direct photon data in the 20% most central Au + Au collisions. In contrast to the others, the curve of F. M. Liu *et al.* [16] includes contributions from pQCD. The black solid curve show the T_{AA} scaled pQCD calculation [11].